

# Behavior of Two Parallel Strip Footings on a Sand Cushion over Clay

Mostafa El Sawwaf <sup>1</sup>, Ashraf K. Nazir <sup>1</sup>, Ahmed Farouk <sup>1</sup>, and Shima Saied <sup>2</sup>

<sup>1</sup> Structural Eng. Department, Faculty of Engineering, Tanta University, Tanta, Egypt

<sup>2</sup> M.Sc. Student, Faculty of Engineering, Tanta University, Tanta, Egypt

Email: [Mostafa.elsawwaf@f-eng.tanta.edu.eg](mailto:Mostafa.elsawwaf@f-eng.tanta.edu.eg), [Ashraf.Nazir@f-eng.tanta.edu.eg](mailto:Ashraf.Nazir@f-eng.tanta.edu.eg),  
[drafarouk@f-eng.tanta.edu.eg](mailto:drafarouk@f-eng.tanta.edu.eg), [Shimaasaied164@gmail.com](mailto:Shimaasaied164@gmail.com)

**Abstract-** In this paper, the behavior of two parallel strip footings resting on the surface of a semi-infinite clay is investigated. The effect of stress interference on bearing capacity and settlement are studied using the finite element program PLAXIS 2D. The clay is stimulated using the Mohr–Coulomb soil model that follows linear-elastic perfectly plastic behavior. A parametric study is performed for different clear spacing between the footings. The paper also presents the effect of existence of a sand cushion as well as the existence of a layer of geogrid inside the cushion below the clay; on the stress-settlement relationship, and the bearing capacity of soil. The results are presented in terms of non-dimensional factors defined as the ratio of settlement and bearing capacity of interfering strip footings to that of a single strip footing resting over the same soil conditions. The study shows that the bearing capacity decreases with the decrease in clear spacing between the parallel strip footings, while the settlement is found to increase. The results of this paper may guide engineers on how to include the effect of spacing between strip footings in the design for a given value of the soil bearing capacity.

**Keywords:** Interference, Strip Footings, Clay, Sand Cushion, Geogrid, PLAXIS 2D.

## I INTRODUCTION

The high need of many construction sites, and rapid urbanization requires to put the foundations or group of foundations very close to each other. Such situations may lead to interference phenomenon in the stress zones below the foundations, which may overlap each other and as a result affect the failure mechanism, settlement and bearing capacity responses of these foundations.

The observation of such phenomenon was first reported by Stuart (1962); who carried out a study using limit equilibrium method on ultimate bearing capacity of two parallel spaced strip footings resting on the surface of cohesionless soil. Nainegali (2013a) put a spotlight on the possibility of using numerical and experimental analysis for simulating the interference of nearby isolated footings resting on nonhomogeneous soil beds. Thereafter, many researchers (e.g., Srinivasan and Ghosh 2013; Nainegali et al. 2013b; Eltohamy and Zidan 2013; Naderi and Hataf 2014; Noorzad and Manavirad 2014; Ghosh et al. 2015; Dhiraj, Yogendra, and Sanjay 2018; Anupkumar and Lohitkumar 2019; Nainegali and Ekbot. 2019; and Anupkumar and Lohitkumar 2021) reported different aspects of the same problem. Subsequently, they observed that the ultimate bearing capacity of the interfering foundations increases with the decrease in spacing and attains a peak at certain critical spacing and the same is true for settlement at failure.

However, from the literature it could be noticed that many

researches were carried out for interfering foundations resting on sand, while very few studies were done for investigating foundations resting on clay. Moreover, nearly no attempts were carried out for studying the interference for foundations resting on improved clay. Henceforth, this research is carried out to observe the effects of interference on two parallel strip footings resting on surface of improved and non-improved clay soil.

## II. PROBLEM DEFINITION

Figure 1 shows two parallel symmetrical strip footings of width ( $b$ ) = 1.0m placed at a clear spacing, ( $s$ ) loaded simultaneously with a uniform stress intensity, ( $q$ ), while resting over a semi-infinite, homogenous reinforced clay soil. The analysis for this study were performed on three different cases. The first is concerned with the performance of parallel strip foundations resting on a layer of clay. In the second case, the strip foundations rest on a sand cushion over the clay layer. The third case is similar to the second case except for the existence of a layer of geogrid embedded inside the sand cushion at a depth equals eighth the sand cushion thickness. The analyses are performed for each case by varying the clear spacing ratio ( $s/b$ ) between the footings. In this study, the effect of stress interference on the bearing capacity, and the settlement of footings against the clear spacing is investigated considering the parameters presented in Tables 1 and 2, respectively.

## III. FINITE ELEMENT MODELING

The analyses in this study are performed considering a plane strain condition, since the length of the strip footing is relatively long when compared to its width. The finite element software PLAXIS 2D is used for modeling two parallel surface strip footings resting on a homogenous semi-infinite clay deposit.

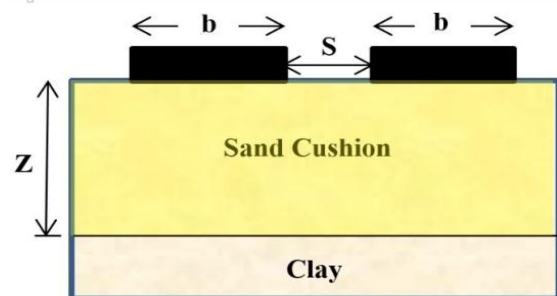


Fig. 1: Model of two parallel strip footings on soil.

Table 1: Material Properties of Clay Soil

Parameters	Values
Material model	Mohr -Coulomb
Material type	Undrained
Unsaturated unit weight ( $\gamma_{\text{unsat}}$ ) in $\text{kN/m}^3$	16
Saturated unit weight ( $\gamma_{\text{sat}}$ ) in $\text{kN/m}^3$	17
Young's modulus ( $E_{\text{ref}}$ ) in $\text{kN/m}^2$	4000
Poisson's ratio ( $\nu$ )	0.35
Cohesion ( $c$ ) in $\text{kN/m}^2$	30
Angle of internal friction ( $\Phi$ ) degree	0
Angle of Dilatancy ( $\psi$ ) degree	0
Interface reduction factor ( $R_{\text{int}}$ )	1

Table 2: Material Properties of Sand Soil

Parameters	Values
Material model	Mohr -Coulomb
Material type	Drained
Unsaturated unit weight ( $\gamma_{\text{unsat}}$ ) $\text{kN/m}^3$	17
Saturated unit weight ( $\gamma_{\text{sat}}$ ) in $\text{kN/m}^3$	18
Young's modulus ( $E_{\text{ref}}$ ) in $\text{kN/m}^2$	75000
Poisson's ratio ( $\nu$ )	0.35
Cohesion ( $c$ ) in $\text{kN/m}^2$	0.1
Angle of internal friction ( $\Phi$ ) degree	40
Interface reduction factor ( $R_{\text{int}}$ )	0.7

The soil is considered to obey Mohr–Coulomb model that follows linear-elastic perfectly plastic behavior. The footings were considered to be rigid by following the procedure described in the PLAXIS tutorial manual, which illustrates that this criterion can be simulated by loading the footings using a prescribed displacement of 1.0 m. This can be achieved by applying this uniform indentation in steps at the top of the soil layer instead of modelling the footing itself. The soil is discretized using 15-noded triangular elements in association with very fine meshing near the vicinity of the simulated footings as shown in Figs. 2 and 3.

Both vertical and horizontal displacements are restricted for the bottom boundary, while the horizontal displacements are restricted for the vertical side boundaries. Prior to calculation, initial stresses of the soil due to its own weight have been generated using the  $K_0$  procedure based on Jacky's formula ( $K_0 = 1 - \sin \phi$ ). Finally, it is to be mentioned that the groundwater level was considered to be 4.0 m below the ground surface.

#### IV. VALIDATION

In the beginning, the finite element model was validated using the model of one strip surface footing, which was simulated in 2019 by Naingali and Ekpote using the PLAXIS 2D program. They reported that the footing is modelled using the plate element. The soil properties adopted in their model are illustrated in Table 3. The footing material is reinforced concrete. Hence, the footing is modelled using linear elastic nonporous type of material, with Young's modulus,  $E = 2.496\text{E}7 \text{ kN/m}^2$  and Poisson's ratio,  $\nu = 0.2$ , bending

stiffness,  $EA = 2.35\text{E}8 \text{ kN/m}$  and axial stiffness,  $EI = 1.958\text{E}7 \text{ kN.m}^2/\text{m}$ .

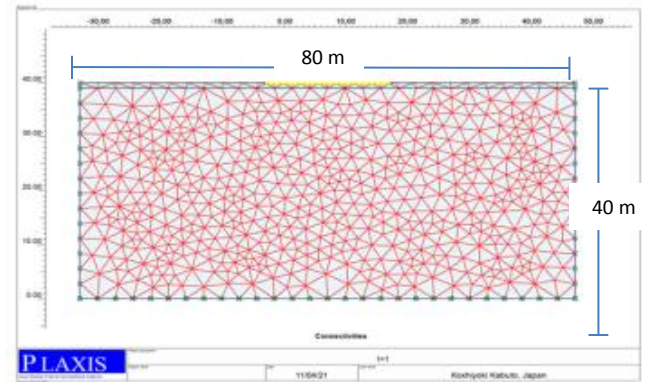


Fig. 2: The mesh of FE modeling of two strip footings on semi-infinite homogenous clay soil.

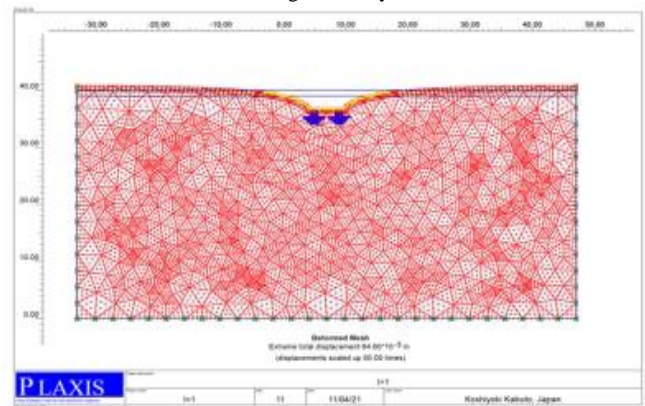


Fig. 3: The geometry of deformed mesh.

Table 3: Properties of soil adopted for the validation model (after Naingali and Ekpote, 2019).

Parameters	Values
Material model	Mohr -Coulomb
Material type	Undrained
Unsaturated unit weight ( $\gamma_{\text{unsat}}$ ) $\text{kN/m}^3$	16
Saturated unit weight ( $\gamma_{\text{sat}}$ ) in $\text{kN/m}^3$	17
Young's modulus ( $E_{\text{ref}}$ ) in $\text{kN/m}^2$	2000
Poisson's ratio ( $\nu$ )	0.3
Cohesion ( $c$ ) in $\text{kN/m}^2$	40
Angle of internal friction ( $\Phi$ ) degree	0
Angle of Dilatancy friction ( $\psi$ ) degree	0
Interface reduction factor ( $R_{\text{int}}$ )	1

The results show that the ultimate bearing capacity (UBC) of a surface strip footing obtained from the present finite element analysis is nearly  $190 \text{ kN/m}^2$ , which matches good with  $UBC = 215.6 \text{ kN/m}^2$  obtained by (Naingali and Ekpote, 2019) considering the same soil and foundation properties, as seen in Fig. 4.

#### V. FINITE ELEMENT RESULTS

Stress–settlement curves are plotted to investigate the variation of bearing capacity of the underneath soil at different ( $s/b$ ) ratios ( $s/b = 0, 0.5, 1, 2$ , and  $3$ ) for two loaded paralleled strip footings.

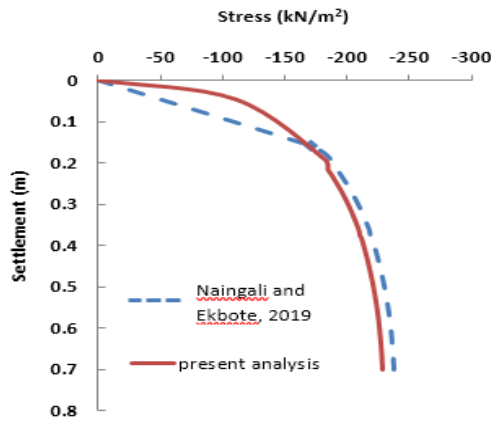


Fig. 4: Validation of Modelling strip footings using PLAXIS 2D.

Figure 5 presents the variation of bearing capacity with the spacing between strip footings resting on clay. The figure shows that the ultimate bearing capacity below one strip footing is very close to that of two parallel strip footings for ratios of ( $s/b=2$ ) and ( $s/b=3$ ). It can be seen that at ( $s/b=3$ ) the behavior of two strip footings seemed to be very close to that of one strip footing.

Figures (6), (7), and (8) show the stress-settlement relationships under two parallel strips of different ratios  $s/b$ . The footings are resting over clay improved with 1.0, 2.0, and 3.0 m of sand cushion, respectively. To illustrate the interference effect, the same figures also contain the stress-settlement relationships below one strip footing resting on the same soil stratigraphy. Figure (6) shows the relationship in case of a top sand cushion having a thickness of 1.00 m. As expected, the figure illustrates that as the spacing between the foundations decreases, the bearing capacity of the soil decreases as well due to the interfering effect.

It can be noticed that at a spacing ratio of ( $s/b=3$ ), the bearing capacity value became 455.56 kPa, which is a value that nearly equals the bearing capacity of a single strip footing (459.09 kPa). Figures 7 and 8 also show the same trend in case of  $z=2.0\text{m}$ , and  $z=3.0\text{m}$ . However, it can be noticed that in the case of a sand cushion of a thickness  $z=3.0\text{m}$  the bearing capacity below the two parallel footings at a spacing ratio of ( $s/b = 2$ ) became (608.5 kPa), which is nearly equal to that below a one strip footing (610 kPa).

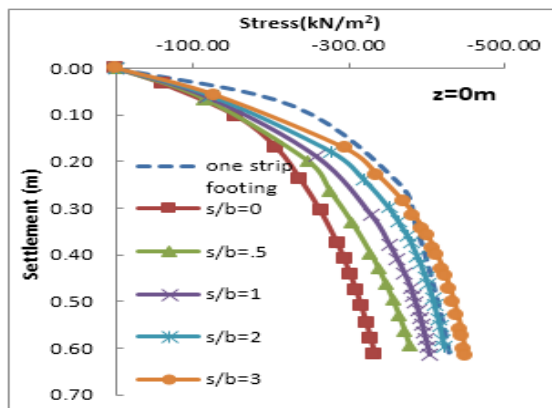


Fig. 5: Stress-settlement curve for strip footings over clay.

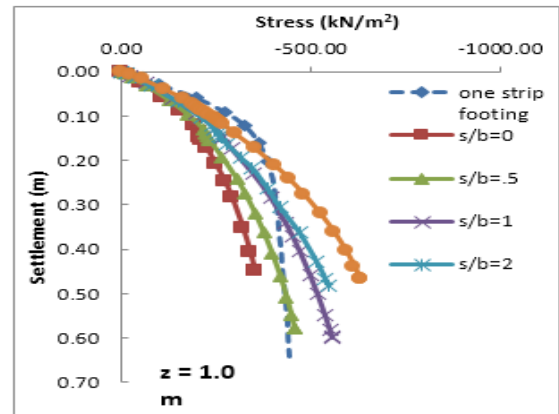


Fig. 6: Stress-settlement curve for strip footing over clay improved with 1.0 m of s and cushion.

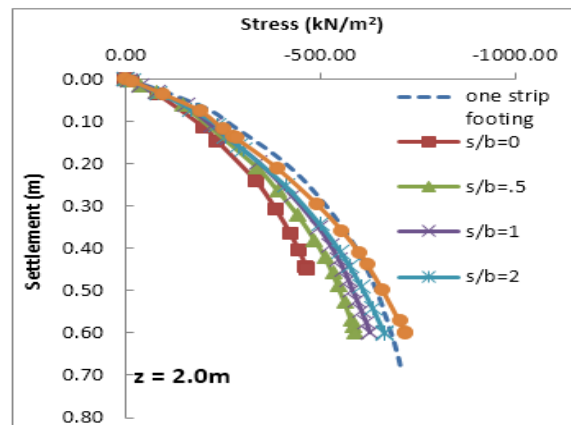


Fig. 7: Stress-settlement curve for strip footing over clay improved with 2.0 m of sand cushion.

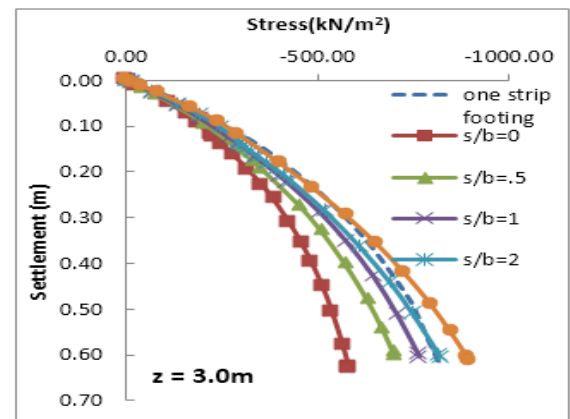


Fig. 8: Stress-settlement curve for strip footing over clay improved with 3.0 m of sand cushion.

This behavior clearly shows that increasing the thickness of a sand cushion leads to vanishing the interference effect at spacing ratios ( $s/b$ ) lower than those required for sand cushions with lower thicknesses. This can be attributed to the fact that as the sand cushion thickness increases, it behaves as a rigid slab below the footing and hence redistributes the stresses into the underlying clay layer.

Figures 9, 10, and 11 illustrate stress-settlement curves for strip footing resting on 1.0, 2.0, and 3.0m of sand cushion,

respectively, reinforced with a layer of geogrid over clay. The geogrid has a normal stiffness (EA) of 100000 kN/m. It was modelled using the geogrid element built in the PLAXIS program.

From the figures it can be seen that the stress-settlement curves became closer to each other as compared to the stress-settlement curves for sand cushion without reinforcement. Besides, the increase of UBC in case of using the geogrid inside sand cushion with a thickness of ( $z = 1\text{m}$ ) is not as big as in case of using it for ( $z = 2\text{m}$  and  $z = 3\text{m}$ ). Also, the UBC value for two parallel strip footings at ( $s/b=3$ ) is very close to the value of one strip footing.

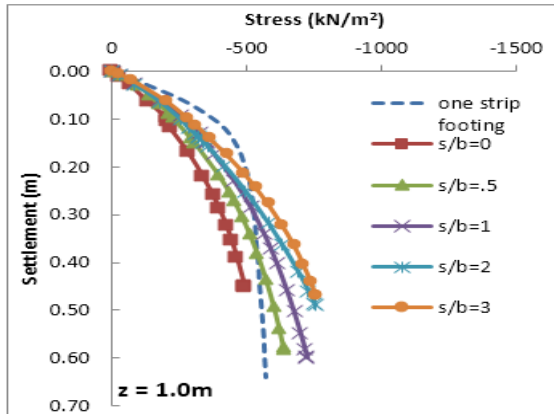


Fig. 9: Stress-settlement curve for strip footing resting on 1.0m of sand cushion reinforced with a layer of geogrids over clay.

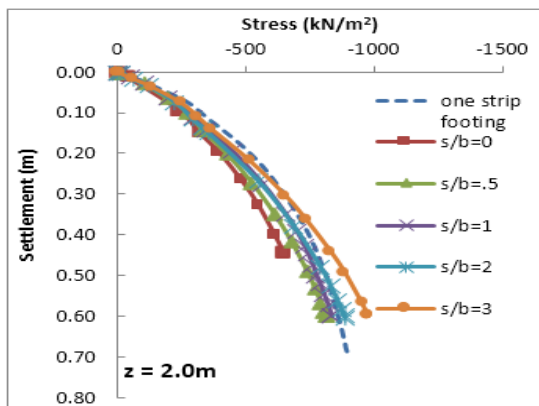


Fig. 10: Stress-settlement curve for strip footing resting on 2.0m of sand cushion reinforced with a layer of geogrids over clay.

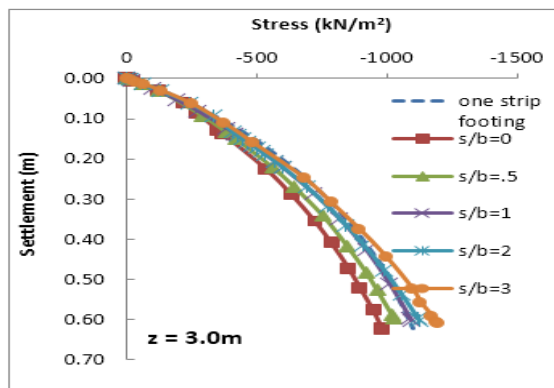


Fig. 11: Stress-settlement curve for strip footing resting on 3.0m of sand cushion reinforced with a layer of geogrids over clay.

## VI. DISCUSSION

In this discussion, the interference in contact stresses below the two parallel strip footing is represented in terms of variation of Ultimate Bearing Capacity Ratio (UBCR). The UBCR is defined as the ratio of the ultimate bearing capacity of soil below two parallel strip footings to the ultimate bearing capacity below only one strip footing.

$$\text{Hence, } UBCR = \frac{BCR \text{ below two parallel strip footings}}{BCR \text{ below one strip footing}}$$

The ultimate bearing capacity (UBC) below footings is quantified using the method of tangents intersection, which is described by Rahman et al. 2003. In this method, tangent lines are drawn from the initial and end points of the stress-settlement curve and the point of intersection of these tangents was projected back to the x-axis to obtain the ultimate bearing capacity. Then, the values of UBCR are plotted against the ( $s/b$ ) ratio for all underneath soils.

Figure 12 illustrates the variation of ultimate bearing capacity ratio (UBCR) below a sand cushion of different thicknesses ( $z$ ) versus the spacing ratio between the strip footings. The figure shows that the UBC below two tangent strip footings (i.e.,  $s/b = 0$ ) is nearly half of that below one footing. It can be seen also, that as the spacing between the footings ( $s/b$ ) increases, the UBCR increases rapidly up to a value of nearly ( $s/b = 0.5$ ), after which the UBCR increases at a slow rate.

Figure 12 shows also that the UBCR becomes unity (i.e., there is no interference in the stresses below the two parallel strip footings) at a spacing ratio of ( $s/b = 3$ ) when the footings rest over a sand cushion with a thickness of 1.0 m. For the sand cushion of a thickness ( $z$ ) equals 2.0 and 3.0 m, the UBCR reaches unity at values of ( $s/b = 2.4$  and  $2.0$  respectively). This proves again that as the sand cushion thickness increases, the interfering effect vanishes at low values of spacing ratios.

Figure 13 shows the variation of UBCR with spacing ratio ( $s/b$ ) in case of embedding a layer of geogrid inside the sand cushion. It can be noticed that the thickness of reinforced sand cushion has a significant effect on the UBCR at spacing ratios ( $s/b$ ) less than 3. However, such effect becomes nearly insignificant at a spacing ratio of 3. Figure (13) illustrates also that increasing the sand cushion thickness from 2.0m to 3.0m has low effect in increasing the UBCR for all values of ( $s/b$ ).

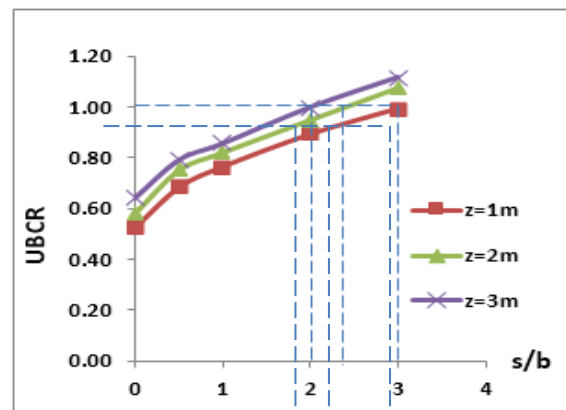


Fig. 12: Variation of UBCR with spacing between footings ( $s/b$ ) resting over different thicknesses ( $z$ ) of a sand cushion replacement.

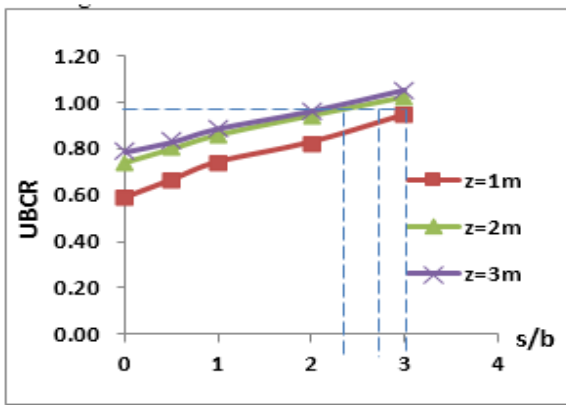


Fig. 13: Variation of UBCR with spacing ( $s/b$ ) between strip footings resting over a reinforced sand cushion.

In addition, the figure shows that the UBCR reaches unity at values of ( $s/b$ ) = 3.0, 2.75, and 2.3 at sand cushion thickness ( $z$ ) of 1.0, 2.0, and 3.0 m, respectively. On the other hand, a comparison between the graphs shown in Figs. 12 and 13 clarifies that the existence of a geogrid increases the values of spacing ratio ( $s/b$ ) at which the UBCR becomes unity. This shows that according to the nature of continuous geogrid in the system, it increases the interfering effect on stresses and deformation.

Figures 14, 15, and 16 show the percentage increase of the UBCR against the spacing ratio ( $s/b$ ) for different depths of a replaced sand cushion over the clay. The figures show that when the two strip footings are tangent (i.e.,  $s/b = 0$ ), the bearing capacity of the soil below the footings are in the range of 53% to 64% of the bearing capacity below an only one footing. However, as the spacing between the footings increases the bearing capacity increases as well. At a spacing ratio of ( $s/b = 3$ ), the bearing capacity below the parallel footings becomes equal to (100%) or even higher (111%) than the bearing capacity below the one footing. It is to be noted that a value of UBCR higher than 100% can be attributed to the effect of the mesh coarseness that is automatically done by the program in case of modelling two parallel footings which might vary from the case of modelling only one footing. Another interpretation is contributed to the soil confinement that increases due to closeness of footings. Also, this can be due to the soil-footing interaction which might vary between the case of modelling one footing and the case of modelling parallel two footings. However, as can be seen, the maximum tolerance is of only 11%.

Figures 17, 18, and 19 show the percentage increase of the UBCR against the spacing ratio ( $s/b$ ) for different depths of a replaced sand cushion reinforced by one layer of geogrid over the clay. The figures show that when the two strip footings are tangent (i.e.,  $s/b = 0$ ), the bearing capacity of the soil below the footings are in the range of 59% to 80% of the bearing capacity below an only one footing. However, as the spacing between the footings increases the reduction in the bearing capacity begins to decrease. At a spacing ratio of ( $s/b = 3$ ), the bearing capacity below the parallel footings becomes nearly equals (100%). However, the variation between the UBCR with the spacing ratio ( $s/b$ ) is not as clear as in the case of using sand cushion only without geogrids reinforcement.

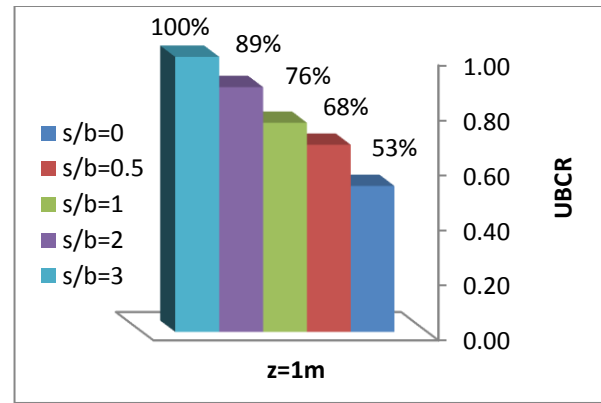


Fig. 14: The percentage increase of the UBCR for different spacing ratio ( $s/b$ ) in case of a replaced sand cushion of ( $z = 1$ m).

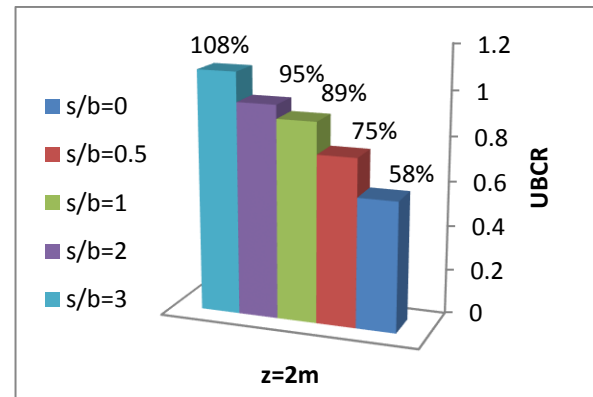


Fig. 15: The percentage increase of the UBCR for different spacing ratio ( $s/b$ ) in case of a replaced sand cushion of ( $z = 2$ m).

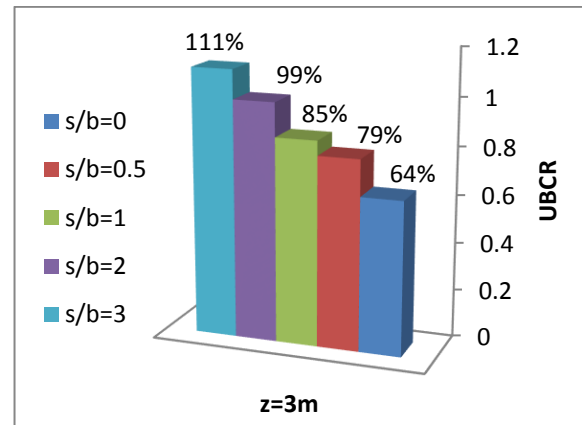


Fig. 16: The percentage increase of the UBCR for different spacing ratio ( $s/b$ ) in case of a replaced sand cushion of ( $z = 3$ m).

Also, it can be noticed that as the thickness of the sand cushion increases the variation decreases. This behavior can be due to the redistribution of the interfering stresses inside the geogrid layer that reinforce the sand cushion.

At a spacing ratio of ( $s/b = 3$ ), the bearing capacity below the parallel footings becomes nearly equals (100%). However, the variation between the UBCR with the spacing ratio ( $s/b$ ) is not as clear as in the case of using sand cushion only without geogrids reinforcement. Also, it can be noticed that as the thickness of the sand cushion increases the variation decreases. This behavior can be due to the redistribution of the interfering

stresses inside the geogrid layer that reinforce the sand cushion.

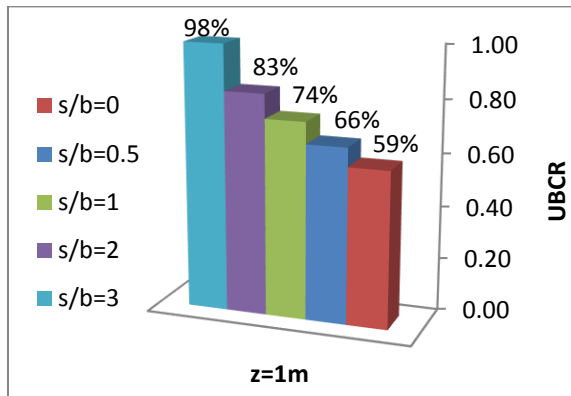


Fig. 17: The percentage increase of the UBCR for different spacing ratio (s/b) in case of a replaced reinforced sand cushion of (z = 1m).

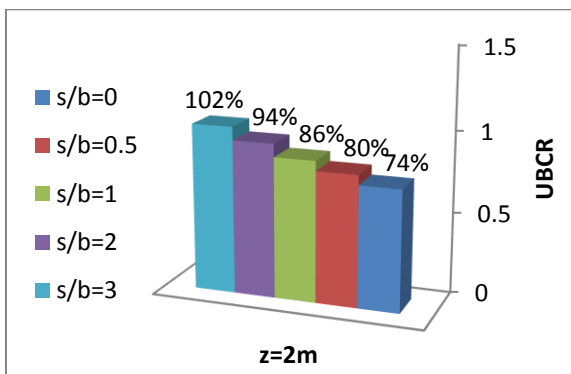


Fig. 18: The percentage increase of the UBCR for different spacing ratio (s/b) in case of a replaced reinforced sand cushion of (z = 2m).

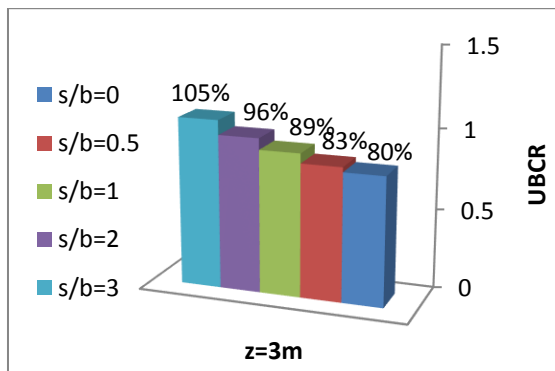


Fig. 19: The percentage increase of the UBCR for different spacing ratio (s/b) in case of a replaced reinforced sand cushion of (z = 3m).

## VII. CONCLUSION

The interference of stresses below two parallel strip footings resting on surface of clay layer as well as on reinforced and non-reinforced sand cushion is investigated in this study using the finite element program PLAXIS 2D. The following conclusions can be extracted from the analysis of results:

1. The ultimate bearing capacity of the clay and sand cushion is affected by the spacing between the parallel strip footings.

2. As the spacing between the two parallel strip footings becomes small, the bearing capacity of the underneath soil becomes small too due to the interfering effect of the stresses below the footings.
3. The interfering effect on both the clay and the sand cushion becomes in general nearly null at a spacing ratio of (s/b=3) between the two parallel strip footings.
4. The ultimate bearing capacity ratio (defined as the ratio of the ultimate bearing capacity of two parallel strip footings to that of one strip footing) increase as the spacing between the footings increases.
5. Increasing the thickness of a sand cushion leads to vanishing the interference effect at spacing ratios (s/b) lower than those required for sand cushions with lower thicknesses.
6. Geotechnical and foundations designer engineers should take into consideration the interference effect of parallel strip footings which might decrease the calculated ultimate bearing capacity of clay by a value of 50% in case of relatively tangent parallel strip footings .

## REFERENCES

- [1] Anupkumar Gopalrao Ekbote & Lohitkumar Nainegali (2021) "Influence of Different Seismic Loadings on the Closely Spaced Interfering Footings Embedded in Cohesionless Foundation Medium" seismic design and performance, Springer, LNCE vol. 120, pp55-73.
- [2] Anupkumar Gopalrao Ekbote & Lohitkumar Nainegali September (2019) "Finite element analysis of two nearby interfering asymmetric footings embedded in cohesionless foundation medium " Geomechanics and Geoengineering 16(5).
- [3] Dhiraj Raj, S.M.ASCE; Yogendra Singh, M.ASCE; and Sanjay K. Shukla, (2018) "Seismic Bearing Capacity of Strip Foundation Embedded in c-φ Soil Slope" International Journal of Geomechanics, volume 18 issue 7.
- [4] Eltohamy, A. M., & Zidan, A. F. (2013), "Performance of interfering strip footings resting on reinforced sand under uniform and non-uniform load-experimental and numerical study". Journal of American Science, 9(1), 421–430.
- [5] Ghosh, P., Basudhar, P. K., Srinivasan, V., and Kunal, K. (2015) "Experimental studies on interference of two angular footings resting on surface of two-layer cohesionless soil deposit" International Journal of Geotechnical Engineering, 9(4), 422–433.
- [6] Naderi, E., and Hataf, N. (2014), "Model testing and numerical investigation of interference effect of closely spaced ring and circular footings on reinforced sand" Geotextile and Geomembranes, 42(3), pp. 191–200
- [7] Nainegali L., Ekbote A.G. (2019) "Interference of Two Nearby Footings Resting on Clay Medium". Geotechnical Applications. Pp.59-67 Springer, Singapore.
- [8] Nainegali, L. S., Basudhar, P. K., & Ghosh, P. (2013), "Interference of two asymmetric closely spaced strip footings resting on nonhomogeneous and linearly elastic soil bed". International Journal of Geomechanics, 13(6), pp.840–851.
- [9] Nainegali L. and Ekbote A. G. Nainegali, L. S. Ghosh, P., and Basudhar, P. K. (2013b). "Interaction of nearby strip footings under inclined loading". Proceedings of the 18th International Conference on Soil Mechanics and Geotechnical Engineering, Paris. Pp.58–66.
- [10] Noorzad, R., and Manavirad, E. (2014), "Bearing capacity of two close strip footings on soft clay reinforced with geotextile" Arabian Journal of Geosciences, 7(2), pp. 623–639.
- [11] PLAXIS (2002), PLAXIS 2D [software]. (Version 8, Finite Element Code for Soil and Rock Analyses). P.O. Box 572, 2600 AN DELFT, Netherlands.
- [12] Rahman, M. M., Alim, M. A. and Chowdhury, M. A. S., (2003) "Investigation of lateral load resistance of laterally loaded pile in sandy soil". Proceedings of the 4th international conference on bored and auger piles, BAPIV, Ghent, Belgium, pp. 209–215.
- [13] Stuart, J. G. (1962). Interference between foundations with special reference to surface footings on sand. Geotechnique, 12(1), pp. 15–23.